Adaptive method for swell noise attenuation in the time-frequency domain

Julio Valença Tavares*, LENEP/UENF, Brazil
Luiz Geraldo Loures, LENEP/UENF, Brazil

Abstract

Coherent noises are those that appear through a systematic way and swell noise is a kind of coherent seismic noise. This happens during the marine seismic acquisition and is generated basically by the motion of the ship, cable depth controllers, or sea surface waves. For the swell noise analysis and attenuation we used a one dimensional wavelet transform, in the sense that it operates on single traces, to apply a time-frequency domain filter. The shifting (time) and level (frequency) dependent soft-threshold is estimated using a method based on Bayes' Rules. Using this proposed methodology for synthetic data analysis the results were satisfactory. When real seismic data is used the results show good agreement due to the algorithm adaptive structure. The noise is removed considerably and the signal doesn't loose the interesting information, validating the proposed model. As the algorithm makes the threshold estimation in function of the scale and for each trace time interval, nine threshold values are calculated for each trace. Therefore, it is possible to reduce the noise for different signal-to-noise ratios (SNR) along each trace. The noise free traces don't change, because in those cases the threshold tends to be zero making possible the perfect signal reconstruction. However, when the SNR tends to be one or the noise and signal amplitude and frequency are similar their coefficient variances tend to be close causing a threshold estimation enough to mute the signal. In agreement with the increasing demand for offshore exploration, also driven by 4D seismic acquisitions, the swell noise will be a frequent problem, because in order to achieve a good geologic model all the distortions generated by the data acquisition should be attenuated.

Introduction

During the marine seismic acquisitions, the swell noise is a type of coherent noise generated by motion of the ship, cable depth controllers, or sea surface waves. Sometimes the swell noise is so strong that we couldn't identify the signals from the data. In agreement with the increasing demand for offshore exploration the swell noise has been researched, besides to predict the noise behavior depending on the environmental conditions and survey design, it can be seen in Martin et al. (2000), Mougenot et al. (2004) e Shepherd and Mcdonald (2004).
According to Yilmaz (2000) a low-cut filter often removes the swell noise from shot records. Some work were developed to coherent seismic noises attenuation using wavelet based techniques, as Duval and Galibert (2002) and Yu and Whitcombe (2008). Deighan et al. (1998) discussed the application of the wavelet packet transform for marine wave swell noise and demonstrated that the noise is concentrated in the lower scales of the wavelet. The simplest filter is used to fill those coefficients in each scale that are significantly affected by the noise with zeros and then carry out the inverse transform. Information is lost where there is an overlap between signal and noise at the low scales. Using common depth point (CDP) gathers after normal move (NMO) out correction, Watts et al. (1999) transformed NMO corrected CDP gathers to the wavelet packet domain using the same idea described above and detect the transformed coefficients corresponding to the wave swell noise using a normalized cross correlation. The data is stacked in the wavelet domain by summing and weighting only those coefficients that most likely correspond to reflections. They lost signal information; nevertheless it showed an improvement in the quality of the stack of a real 2-D marine data set with the application of this method.

In this paper, we proposed a methodology to swell noise attenuation in the time-frequency domain, using an adaptive method for the threshold estimation. This method, called BayesShrink (Chang et al., 2000). As the wavelet transform makes possible the time-frequency domain analysis, each trace was divided in three time intervals to suppress the noise to different signal-to-noise ratios (SNR). The algorithm input data is the seismogram, a mother wavelet and the first break of each trace. All the traces that will be analyzed are divided after the transform in three time intervals, in agreement with the first break. Due to the algorithm adaptive structure, nine threshold values were computed, being able to reduce noise from different SNR. We obtained good results using this methodology in synthetic data and when applied in real seismograms the results were suitable. The noise is considerably removed and the signal doesn't loose the interesting information, validating the proposed model.

One dimensional discrete wavelet transform

Mathematically speaking, the wavelet transform is a convolution of the wavelet function with the signal. If, however, the wavelet and the signal do not correlate well, a low value of the transform is obtained (Addison, 2002). Doing this at various locations of the signal and for various scales of the wavelet, we could plot the wavelet transform coefficients as a picture to be built up the correlation between the wavelet and the signal. The wavelet transform can be expressed as

$$Y(m,n) = \langle S, \psi_{m,n} \rangle$$

where *Y* is the wavelet transform coefficient for the scale m and location n. S is the signal and ψ the wavelet function.

The discrete wavelet transform (DWT) divides the signal in high scales and low scales components, called approximation and details coefficients, respectively. The approximation coefficients return the low frequency component of the signal, and the details correspond to high frequency. This decomposition was done up to the second level to increase the frequency resolution and is represented as a binary tree with nodes representing a sub-space with different time-frequency localization. The tree is known as a filter bank, where a data downsampling is used during the convolution for each level. An example for a data with 1000 samples is shown in Figure 1 to illustrate this procedure.

One type of processing in the wavelet domain is the signal reconstruction rejecting the coefficients with low values, corresponding to the incoherent part of the signal, or the noise. The noise attenuation, or denoising, can be defined as fallows.

If $\mathrm{S(t)}$ is the noisy signal

$$\mathrm{S(t) = x(t) + n(t)}$$

where $\mathrm{x(t)}$ is the free noise data, and $\mathrm{n(t)}$ the additive noise. Choosing an operator $D(.,\tau)$ to represent the denoising, in the threshold τ, an operator $W(.)$ to represent the forward wavelet transform and an operator $W^{-1}(.)$ to represent the inverse wavelet transform, we can simplify this procedure as fallows

$$Y = W(S)$$
$$Y^{*} = D(Y,\tau)$$
$$S'(t) = W^{-1}(Y^{*})$$

where $\mathrm{S'(t)}$ is the estimated free noise data. As it can be seen, after the wavelet decomposition the coefficients are filtered, this filter needs to be previously defined, and it calls wavelet shrinkage. Then carry out the inverse transform to reconstruct the signal. In the next section will be discussed the threshold estimation for wavelet shrinkage.

Threshold estimation for wavelet shrinkage

After the wavelet decomposition, we can change or remove some coefficients, after that, do the signal reconstruction. We can set groups of coefficients to zero or set selected individual coefficients to zero. Also, we can reduce the magnitudes of some coefficients rather than set then to zero. There are many methods for selecting and modifying the coefficients, the two most popular are soft and hard thresholding. Those coefficients above the threshold are deemed to correspond to the coherent part of the signal, and those below the threshold are deemed to correspond to the random or noisy part of the signal. Soft thresholding is of the form

$$Y^{soft} = \begin{cases} 0 & |Y| < \tau \\ sign(Y)\left[|Y| - \tau\right] & |Y| \geq \tau \end{cases}$$

where all coefficients below the threshold, τ, are set to zero and all the coefficients whose magnitude is greater than are shrunken towards zero by an amount τ. The threshold can, for example, be a constant value applied to the coefficients across all scales, some of the scales, or its value can vary according to scale. The last method is called level dependent thresholding.

There are some methods to the threshold estimation, for example: Donoho and Johnstone (1994a), Kaur et al. (2003), Miao and Cheadle (1998), and Nason (1995). In this article was estimated a level dependent soft threshold using a method called BayesShrink, which proposes an adaptive data-driven threshold for signal denoising via wavelet soft-thresholding that was derived in a Bayesian framework, based on prior information about the noise. This information is the noise coefficient variance, σ^2, that needs to be estimated first. Recall the observation model is $\mathrm{S(t) = x(t) + n(t)}$, with x and n independent of each other. In summary, this method uses this idea:

If $\sigma_Y^2 = \sigma_X^2 + \sigma^2$, where σ_Y^2 is the variance of Y. Thus

$$\tau_b(\hat{\sigma}_X) = \frac{\sigma^2}{\hat{\sigma}_X}$$

where $\hat{\sigma}_X = \sqrt{\max(\sigma_Y^2 - \sigma^2, 0)}$. In the case that $\sigma^2 \geq \sigma_Y^2$, $\hat{\sigma}_X$ is taken to be zero. That is, $\tau_b(\hat{\sigma}_X)$ is ∞, or, in practice, $\tau_b(\hat{\sigma}_X) = \max(|Y|)$ and all coefficients are set to zero. This happens at times when σ^2 is large. To summarize, this method performs soft-thresholding, with the data-driven, subband-dependent threshold. In the next section the algorithm structure for the synthetic and real data analysis will be displayed.

Synthetic and real data processing

The DWT was applied, with two decomposition levels, in three traces. A selected real trace, $\mathrm{T_{re}}$, and two synthetic traces. One of these synthetic traces is the one that contains only noise. To achieve this goal, a data sampling is done in $\mathrm{T_{re}}$, before the first break, where there is only noisy. With this sampling, a trace with the same length of the original data is created, $\mathrm{T_{no}}$, just repeating this sample, that will be called as synthetic noisy trace. Choosing a neighboring noise free trace, $\mathrm{T_{nf}}$, we created a synthetic trace, as fallows $\mathrm{T_{sy} = T_{nf} + T_{no}}$.

In summary, for the wavelet analysis will be used T_{re}, T_{sy} and T_{no}. Once, we will show all the procedures for the synthetic data analysis, and then in the end of this section the real data analysis will be discussed.

To execute the time-frequency domain analysis, the wavelet coefficient vector of each trace was divided in three parts, following the same idea; the first time interval correspond to the initial time interval, until de first break, $T(i)$, para $i_1 = 1,2,...,n_{fb}$, where n_{fb} is the first break index. After n_{fb} the trace is divided in two parts, with $i_2 = n_{fb} + 1, ...,[n + (n - n_{fb})/2]$ e $i_3 = n_{fb} + [n + (n - n_{fb})/2] + 1, ..., n$, where n is the length of $T(i)$. Due to downsampling procedure this time sampling is adjusted for each scale. For each T_{sy} and T_{no} interval the approximation and details coefficient variance is estimated. Figure 2 display the approximation and detail coefficient histograms, in agreement with the time intervals, of the synthetic trace and synthetic noisy trace. We can see that for the first part, i_1, the coefficient distribution, between this two traces are similar and it should be. For the second and third parts, i_2 and i_3, the approximation coefficient distribution are so different, confirming what said, that the swell noise is well represented in the detail coefficients. Using the BayesShrink method, the shrinkage was applied. After the shifting and level dependent soft-thresholding, $\tau_b\left(\hat{\sigma}_X^{m,n}\right)$, the synthetic trace is reconstructed, $S'(t) = W^{-1}(Y_{m,n}^{*})$ .Table 1 shows σ_Y^2, \sigma^{2}, σ^2 and $\hat{\sigma}_X$ for each scale and time interval, i_1, i_2 and i_3. Figure 3 displays the coefficient vector for all scales and the dashed line correspond to the threshold value applied for each time interval. Figure 4 shows a crossplotting of T_{sy} and $T_{sy}^{'}$, on the top, and the residual, on the bottom.

Using the same methodology for the real noisy trace, T_{re}, it can be seen in Figure 5, Figure 6, Figure 7 and Table 2, that the proposed model for the synthetic data analyses agree with the real situation. In summary, to use it in a real seismogram, will be necessary to set the algorithm to analyze each trace. For each trace, T_{re}, a noisy synthetic trace, T_{no}, needs to be created. After the transform and the signal processing, each trace is reconstructed.

Results and discussions

In order to better visualize and compare the results, in Figure 8 shows the results for the synthetic trace analysis and Figure 9 shows the results for the real noisy trace, according to the time intervals, i_1, i_2 and i_3.

The proposed algorithm applies this methodology in a real seismogram, analyzing each trace. The results can be seen in Figure 10. A seismogram section highlighted in Figure 10(a) was selected for a better view of the processing results. Figure 11 shows the selected section, (a), the processed section, (b), and the residual, (c).

When the noise and signal, amplitude and frequency, are similar the algorithm tends to calculate a thresholding value enough to cut all the signal, but it happens when the swell noise is so strong that we can't identify the signal from the trace. Thereby, $\sigma_Y^2 \approx \sigma^2$, in that case the estimated signal standard deviation tends to be zero, $\hat{\sigma}_X \approx 0$, consequently $\tau_b(\hat{\sigma}_X) \approx \max(|Y|)$. Figure 12 shows all the traces that was muted.

In the noise free traces, the algorithm doesn't change the signal, therefore T_{no} is generated with its initial time sampling, where there is no signal and noise. So the wavelet transform coefficients will be zero, or very close, then $\sigma^2 \approx 0$, that is $\tau_b(\hat{\sigma}_X) \approx 0$. Thereby, the signal coefficients won't be modified before carrying out the inverse transform.

Just to help in the coefficient interpretation, we applied the continuous wavelet transform in the noise free trace, noisy real trace, synthetic trace and the trace number 319, T_{319} which the noise and signal, amplitude and frequency, are similar. In Figure 13 can be seen that the coefficients related to the swell noise are placed in the low scales of the wavelet and in T_{319} coefficients the noise is well represented in the high scales.

E. Kragh (2002) showed that the reducing tension down the streamer gives an increasing in movement toward the tail end. This movement is coupled to the swell. In Figure 10(a) we can see that the last traces shows more swell noise. As we have shown the swell noise is placed in the low scales of the wavelet transform and starting from this idea it was possible to prove that this situation can be shown using the details coefficient variance. When DWT is applied in the initial time interval, until the first break, of each trace and is computed detail coefficient variance for the first and second decomposition level, it can be seen that the last traces show high variances, it is shown in Figure 14.

Conclusions

Using one dimensional DWT for seismic data containing swell noise, we characterized and attenuated the noise in both synthetic data and real data. Due to the algorithm adaptive structure, nine threshold values were computed, for each trace, being able to reduce noise for different SNR. Notice that the noise free traces don't loose the interesting information, because the threshold tends to be

zero, making it possible that the signal can be reconstructed without loss. This methodology can be applied in any type of sort, thus the algorithm processes each trace independently on the geometry acquisition. The results were suitable and this proposed methodology showed itself robust. In real seismograms, the noise is considerably removed and the signal doesn't loose the interesting information, validating the proposed model.

Acknowledgements

We wish to thank LENEP/UENF and FAPERJ for supporting this research.

References

P.S. Addison, 2002, The Illustrated Wavelet Transform Handbook. IOP Publishing Ltd.

S.G. Chang, B. Yu, and M. Vetterli, 2000, Adaptative wavelet thresholding for image denoising and compression. IEEE Transactions on Image Processing, 9(9): 1532-1546.

A.J. Deighan, D.R. Watts, and C. Riedel, 1998, Wave swell noise suppression using a wavelet packet transform. EAGE 60th International Meeting.

D.L. Donoho and I.M. Johnstone,1994a, Adapting to unknown smoothness via wavelet shrinkage. Technical report, Department of Statistics Stanford University.

L.C. Duval and P.Y. Galibert, 2002, Efficient coherent noise filtering: an application of shift-invariant wavelet denoising. EAGE 64th Conference & Technical Exhibition.

L. Combee E. Kragh, R. Laws, 2002, Sea surface shape derivation above the seismic streamer. Technical report, EAGE 64th Conference & Exhibition, Florence, Italy.

L. Kaur, S. Gupta, and R.C. Chauhan, 2003, Image denoising unsing wavelet thresholding. Technical report, SLIET, Image denoising using wavelet thresholding.

J. Martin, A. Ozbek, L. Combee, N. Lunde, S. Bittleston, and E. Kragh, 2000, Acquisition of marine point receiver seismic data with a towed streamer. Society of Exploration Geophysicists, (Expanded Abstracts).

X. Miao and S. Cheadle,1998, Noise attenuation with wavelet transform. Technical report, Veritas DGC Inc.

J.M. Mougenot, O. Zdraveva, and K. Kravik, 2004, Optimization of swell noise specifications as part of survey design. EAGE Fall Research Workshop on Advances in Seismic Acquisition Technology.

G.P. Nason, 1995, Choice of the threshold parameter in wavelet function estimation. Technical report, Department of Mathematics, University of Bristol.

A.M. Shepherd and J.A. Mcdonald, 2004, Quantification of swell noise on seismic lines gathered in rough and calm seas. EAGE 66th Conference & Exhibition.

D.R. Watts, A.J. Deighan, and C. Riedel, 1999, Attenuation of marine wave swell noise by stacking in the wavelet packet domain. Society of Exploration Geophysicists (Expanded Abstracts).

O. Yilmaz, 2000, Seismic Data Analysis: Processing, Inversion, and Interpretation of Seismic Data, volume 1 of Investigations in Geophysics. Society of Exploration Geophysicists, Tulsa.

Z. Yu and D. Whitcombe, 2008, Seismic noise attenuation using 2d complex wavelet transform. EAGE 70th Conference & Exhibition.

Table 1: Synthetic trace results. Synthetic trace coefficient variance, σ_Y^2, synthetic noisy trace variance, σ^2, estimated standard deviation of the signal, $\hat{\sigma}_X$, and the threshold value applied in each subband and for each trace time interval, τ_b.

Approximation - Level 2				
	σ^2_Y (x10^{-15})	σ^2 (x10^{-15})	σ_x (x10^{-8})	$T_B(\sigma_x)$
i_1	5,77	3,61	4,65	6,55 x10^{-8}
i_2	1340000,00	2,27	3660,00	4,35 x10^{-11}
i_3	27300,00	3,29	523,00	4,64 x10^{-10}
Detail - Level 2				
	σ^2_Y (x10^{-14})	σ^2 (x10^{-14})	σ_x (x10^{-8})	$T_B(\sigma_x)$
i_1	2,95	2,89	2,31	1,25 x10^{-06}
i_2	727,00	3,11	269,00	1,16 x10^{-09}
i_3	13,80	3,00	32,80	9,14 x10^{-08}
Detail - Level 1				
	σ^2_Y (x10^{-14})	σ^2 (x10^{-14})	σ_x (x10^{-8})	$T_B(\sigma_x)$
i_1	3,52	3,46	2,28	1,52 x10^{-06}
i_2	11,20	3,43	28,00	1,23 x10^{-07}
i_3	3,51	3,42	3,02	1,13 x10^{-06}

Table 2: Selected real trace results. Selected real trace coefficient variance, σ_Y^2, synthetic noisy trace variance, σ^2, estimated standard deviation of the signal, $\hat{\sigma}_X$, and the threshold value applied in each subband and for each trace time interval, τ_b.

Approximation - Level 2				
	σ^2_Y (x10^{-15})	σ^2 (x10^{-15})	σ_x (x10^{-9})	$T_B(\sigma_x)$
i_1	3,57	3,57	1,71	2,09 x10^{-6}
i_2	375000,00	2,31	19400,00	1,19 x10^{-10}
i_3	7910,00	3,27	2810,00	1,16 x10^{-9}
Detail - Level 2				
	σ^2_Y (x10^{-14})	σ^2 (x10^{-14})	σ_x (x10^{-9})	$T_B(\sigma_x)$
i_1	2,85	2,85	5,19	5,49 x10^{-06}
i_2	192,00	3,18	1370,00	2,32 x10^{-08}
i_3	6,98	2,97	200,00	1,48 x10^{-07}
Detail - Level 1				
	σ^2_Y (x10^{-14})	σ^2 (x10^{-14})	σ_x (x10^{-8})	$T_B(\sigma_x)$
i_1	3,47	3,44	1,81	1,90 x10^{-06}
i_2	5,62	3,46	14,70	2,35 x10^{-07}
i_3	3,95	3,40	7,39	4,60 x10^{-07}

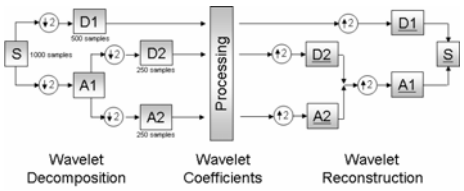

Figure 1: Illustration of wavelet decomposition, processing and wavelet reconstruction.

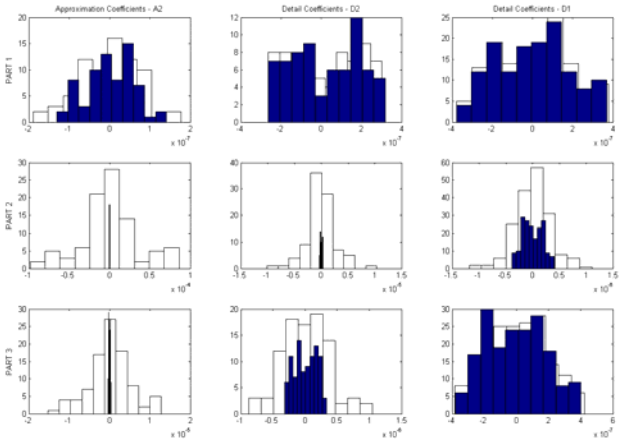

Figure 2: Coefficient histograms, white for T_{sy} and blue for T_{no}.

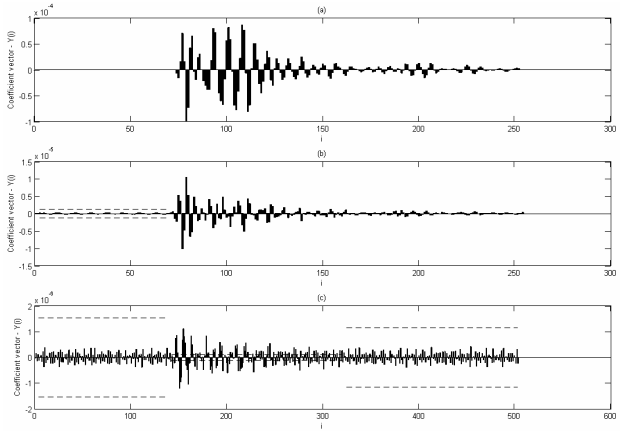

Figure 3: Synthetic trace wavelet coefficients for each scale. (a) Approximation coefficients of the 2nd decomposition level. (b) Detail coefficients of the 2nd decomposition level. (c) Detail coefficients of the 1st decomposition level. The dashed lines correspond to the threshold value for each time interval.

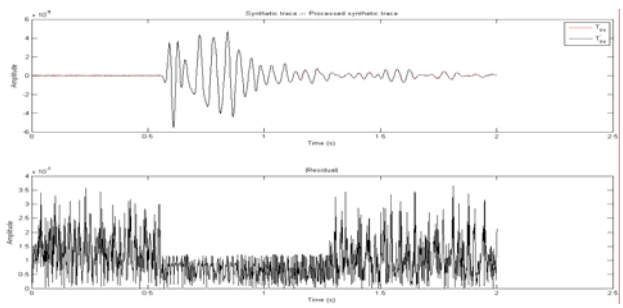

Figure 4: Synthetic trace analysis results.

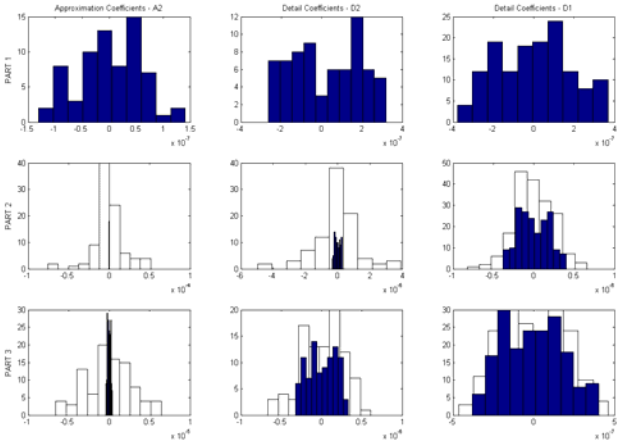

Figure 5: Coefficient histograms, white for T_{re} and blue for T_{no}.

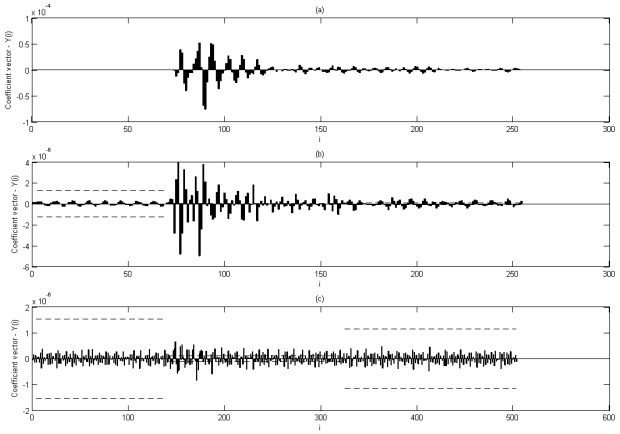

Figure 6: Selected real trace wavelet coefficients for each scale. (a) Approximation coefficients of the 2nd decomposition level. (b) Detail coefficients of the 2nd decomposition level. (c) Detail coefficients of the 1st decomposition level. The dashed lines correspond to the threshold value for each time interval.

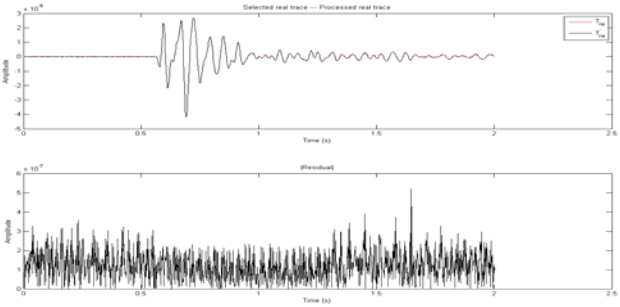

Figure 7: Selected real trace analysis results.

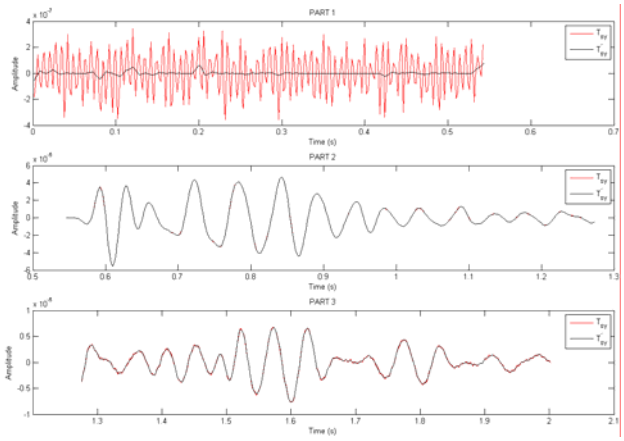

Figure 8: The synthetic trace, T_{sy}, and the processing result, T'_{sy}.

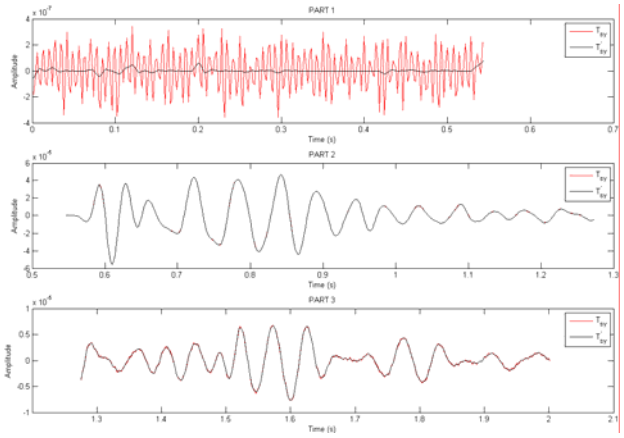

Figure 9: The noisy real trace, T_{re}, and the processing result, T'_{re}.

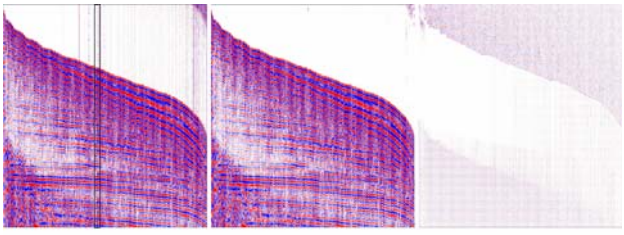

Figure 10: (a) Real seismogram. (b) Processed seismogram. (c) Residual.

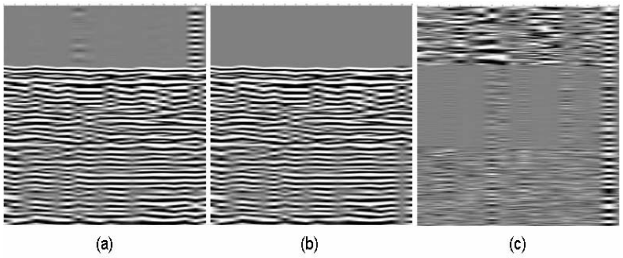

Figure 11: The seismogram highlighted section in Figure 10(a).

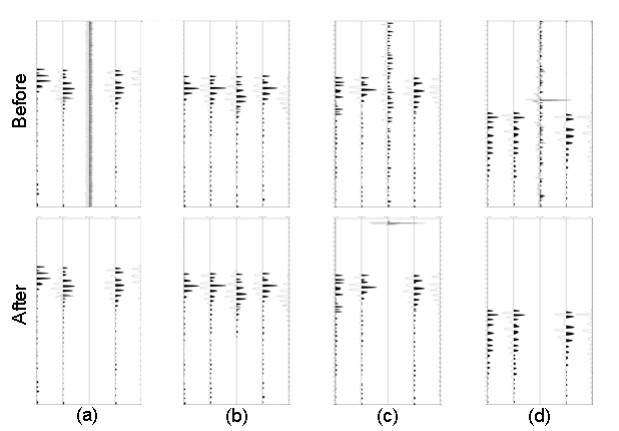

Figure 12: On the top is shown muted traces before the processing, and on the bottom, those traces after the processing. . (a) k=255. (b) k=319. (c) k=327. (d) k=640.

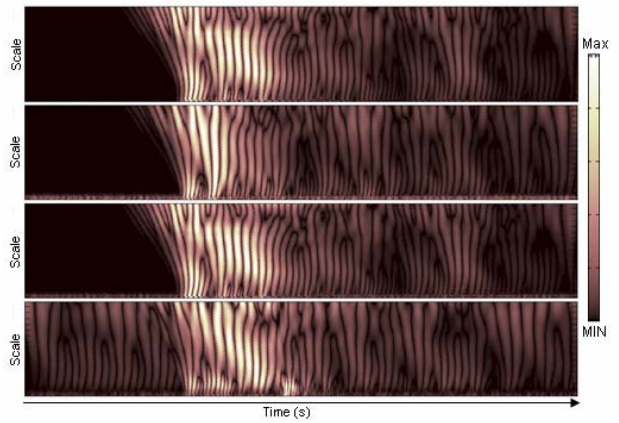

Figure 13: Normalized coefficients of the continuous wavelet transform. From the top to bottom, free noise trace, selected noisy real trace, synthetic trace and trace number 319.

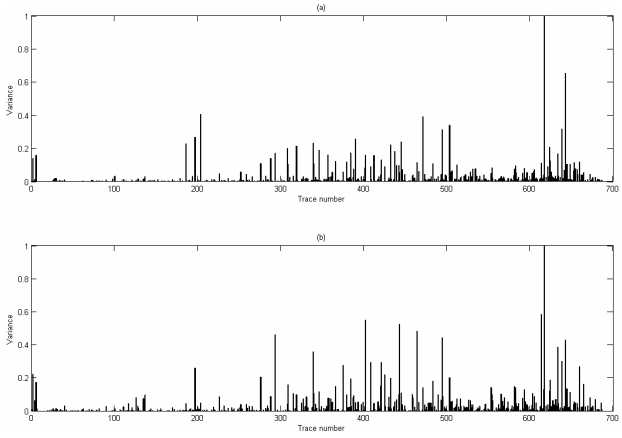

Figure 14: Detail coefficient normalized variance for the second decomposition level, (a), and the first decomposition level (b). It was done for the initial time interval, until the first break, of each trace.